Frequency-Domain Identification of a Ventilated Room for Model Based Control

David Sturzenegger [*,***] Dominik Keusch [*]
Leonardo Muffato [**] Dominique Kunz [**] Roy S. Smith [*]

* Automatic Control Laboratory, ETH Zurich.
** SAUTER AG, Basel, Switzerland.
*** Corresponding author: sturzenegger@control.ee.ethz.ch.

Abstract: Efficient and accurate modeling techniques have become increasingly important in the context of model predictive control (MPC) for building automation. For modeling single-input single-output systems such as a ventilated room (with either constant air flow or constant supply temperature), system identification methods are promising and provide insight into the physical nature of these systems. In collaboration with the company SAUTER an office type test room was instrumented for experiments. Three models for the room were derived: i) an empirical transfer function estimate (ETFE) derived from a pseudo-random binary sequence input signal; ii) an ETFE derived from a relay feedback approach; iii) a physics based resistance-capacitance (RC) model.
Using additional validation data, the different models and approaches were compared in terms of accuracy and efficiency. The effect of air mixing dynamics was demonstrated in an additional experiment to be one of the main differences between the experimentally identified and the RC model. An additional pole can be added to the RC model in order to compensate for the differences.

Keywords: Model predictive control, Building automation, System identification.

1. INTRODUCTION

The application of model predictive control (MPC) for the control of heating, cooling, ventilation and blind positioning in buildings has recently gained much attention within the control community, see e.g. Siroky et al. (2011); Oldewurtel et al. (2012); Ma et al. (2012); Sturzenegger et al. (2013); Bengea et al. (2014).

In a building control context, MPC is often considered as a whole building supervisory control. Nevertheless, it may be interesting (potentially as a first step towards whole building MPC) for single room applications as well. In both cases efficient and accurate modeling techniques are becoming increasingly important since cost effectively generating a model is usually the dominant obstacle.

Two principal ways exist for modeling buildings: identification and physics based approaches. While the former have their benefits, due to time and building usage constraints, it is often impractical or even impossible to excite buildings sufficiently for the identification of multi-input multi-output whole building models as required in a supervisory MPC. For this use we advocate physics based models together with an online adaptation of a few parameters usually related to the faster dynamics of the model.
For single-input control of a room however, identification approaches are an interesting alternative avoiding the physics based approaches' need for construction data.

In this paper we show the results of several experiments conducted in a well instrumented ventilated test room (see Section 2) of the company SAUTER [1]. In the experiments

we fixed the air flow rate to the test room and used a heating device to excite the thermal room dynamics. Section 3 shows the results of the identification experiments. We calculated empirical transfer function estimates (ETFE) on one hand from an experiment with a pseudo-random binary sequence (PRBS) signal as input and on the other hand in a closed-loop identification setup with a relay feedback controller. In Section 4 we show the results of a validation experiment. Using this data we compared several models: the model identified in Section 3; a physics based model generated from construction data; and a modified version of the latter. The modification consisted of an additional pole and compensated for discrepancies found when comparing the identified and the physics based model in the frequency-domain. In Section 5 the results are discussed and conclusions are drawn in Section 6.

2. EXPERIMENTAL SETUP

A rectangular room located at SAUTER's headquarter and production site in Basel was chosen as experimental facility. The system was defined to be the whole room, including the walls, ceiling and floor. Figure 1 shows a map of the room's surroundings. The room comprised a ventilation unit having air inlet and outlet in the nearby control room, a heating device in the supply air duct and ten temperature sensors. Active cooling of the supply air was not possible. All components are illustrated in Figure 2. To avoid excessive heating up of the control room, the door from the control room towards the big storage hall was kept open.

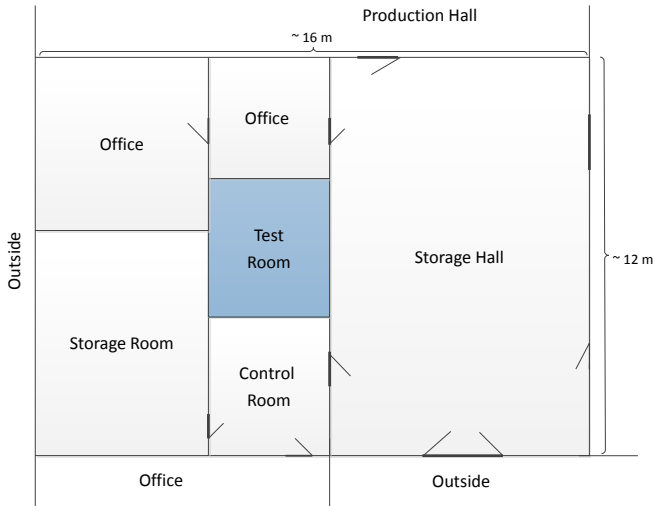[1] http://www.sauter-controls.com (last accessed: March 2014)

Fig. 1. Room surroundings.

Table 1. Temperature sensor locations.

Sensor	Location
T_{amb}	In the control room.
T_{sup}	Supply air duct after the heater.
T_{ret}	Return air duct.
T_{table}	On the table in the center of the room.
$T_{ceiling}$	In the center of the ceiling.
T_{floor}	In the center of the floor underneath the table.
$T_{wall,N}$	In the center of the wall opposite the door.
$T_{wall,W}$	In the center of the wall left from the door.
$T_{wall,E}$	In the center of the wall right from the door.
$T_{wall,S}$	In the center of the wall next to the door.

Actuators. A heating device from the company VEAB Heat Tech AB[3] was used. The device takes as input a 0-10 V signal and produces a pulse width modulated heating power signal with a maximum value of 1800 W. To be able to exactly predict switching times in the identification experiments[4], we decided to modulate the signal ourselves by applying either 0 V or 10 V. These input values resulted in instantaneous changes of the heating power to 0 W or 1800 W, respectively. Our modulation period was chosen to be 20 s. Since the minimum time between two switches of the heating device is 5 s, this modulation was capable of producing 0%, 25%, 50%, 75% and 100% of the maximum heating power. Due to temperature limitations of the heater, it was not possible to use it for a longer period in 75% or 100% mode. Hence, it was subsequently never used more than in 50% mode.

Data Acquisition. For acquiring the sensor measurements a data logger from the company Fluke[5] was used. The sampling time of the data acquisition was set to $t_{\text{samp}} = 10$ s.

3. IDENTIFICATION EXPERIMENTS

The system was mainly influenced by three variables: i) the surrounding air temperature, T_{amb}, influencing the supplied air temperature and the heat gain to the room's outer wall layers; ii) the (volumetric) ventilation air flow rate, $\dot{V}$, and iii) the power of the heating device, $\dot{Q}_{heat}$. The heat gain to the room air from the ventilation can be modeled as

$$C_{air}\rho_{air}\dot{V}T_{amb} + \dot{Q}_{heat} \qquad (1)$$

with C_{air} and ρ_{air} being the heat capacity and density of air at 22 °C, respectively. The heat loss due to the air flow leaving the room was modeled accordingly as

$$-C_{air}\rho_{air}T_{ret}\dot{V}.$$

In the present experiments, $\dot{V}$ was set constant to $\dot{V}_0 = 180$ m^3/h, which corresponds to an air change rate of 5 1/h. This is a typical configuration for a heating case. In this work we considered the system to have just,

$$\Delta\dot{Q}_{heat} := \dot{Q}_{heat} - \dot{Q}_{heat,ss},$$

Fig. 2. Experimental setup. Red dots denote temperature sensor locations.

Temperature Sensors. All temperature sensors have been acquired from the company Innovative Sensor Technology AG[2]. Prior to the system identification, a test was conducted to compare the steady-state measurements and sensor dynamics. The static differences of the sensors were measured to lie within 0.12 °C and the temperature values after a temperature step (but before equilibrium was reached again) were found to differ at most by 0.25 °C. This was sufficiently accurate in the context of the planned experiments. Table 1 details the location of the sensors. The sensors on the walls, ceiling and floor were attached at a distance of approximately 10 cm off the wall to reduce direct influences from the wall temperature.

---

[2] http://www.ist-ag.com (last accessed: March 2014)

[3] http://www.veab.com (last accessed: March 2014)
[4] For the validation experiment, the original modulation was used.
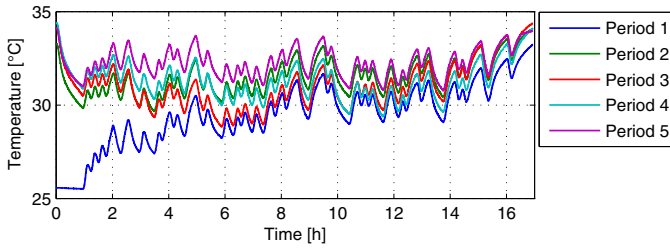[5] http://www.fluke.com (last accessed: March 2014)

Fig. 3. Measurements of sensor T_{table} during the first 5 periods of PRBS Experiment 1.

as a single input and to treat T_{amb} as a disturbance ($\dot{Q}_{heat,ss}$ denotes the steady-state heating power value). However, the direct effect of T_{amb} on the room can be considered by using instead of $\Delta\dot{Q}_{heat}$,

$$\Delta\dot{Q}'_{heat} = \Delta\dot{Q}_{heat} + C_{air}\rho_{air}\dot{V}_0(T_{amb} - T_{amb,ss}), \quad (2)$$

where $T_{amb,ss}$ is the value of T_{amb} at steady-state conditions. The sensor T_{table} was chosen as (main) output since it represents the best approximation to the temperature occupants would feel. In Section 4.4 also the other sensors are considered. In the following, whenever not differently stated, the system is considered to be single-input single-output from $\Delta\dot{Q}'_{heat}$ to $\Delta T_{table} = T_{table} - T_{table,ss}$, with $T_{table,ss}$ being the steady-state temperature corresponding to $T_{amb,ss}$, $\dot{Q}_{heat,ss}$ and $\dot{V}_0$. In a preliminary step response experiment, the dominant time-constant (i.e. the time-constant of the best first order approximation) was identified to be around 168 minutes.

3.1 Identification Using a PRBS Signal

As a first approach we identified the ETFE using a PRBS signal. A PRBS signal is an $n_{periods}$ times repeated periodic signal. Each period consists of $n_{samples}$ intervals of length t_{switch}. The value of the signal during each interval is constant and determined by a (pseudo-)random binary number specifying whether the signal's maximum or minimum value is applied. As discussed in Section 2, there was no cooling device and the maximum heating power was restricted to 50 % peak output, i.e. to 900 W. Hence the signal's minimum and maximum values were 0 W and 900 W, respectively.
The interval length was fixed to $t_{switch} = 480$ s. Choosing $n_{samples} = 127$ resulted in a lowest achievable frequency point $\frac{2\pi}{t_{switch}\cdot n_{samples}} = 1.0307\cdot 10^{-4}$ rad/s, which is lower than the cutoff frequency of the first order approximation and results in a PRBS period of approximately 17 h.

The modulation of the heating device changes the frequency spectrum of the input signal. A coherency analysis taking into account this effect, the maximum PRBS signal frequency and the sampling led to disregarding all frequencies higher than 0.01 rad/s.

Two PRBS experiments were performed, each encompassing 8 periods of 17 h. For the first PRBS experiment the temperature measured by T_{table} during the first five periods is shown in Figure 3. For sake of space, the other periods' and the second experiment's temperature trajectories are not shown. Clearly, period 1 contained most of the transients and was discarded in the further steps. The ETFE was calculated as

$$\hat{G}(j\omega_k) = \frac{Y(k)}{U(k)}, \qquad k = 1...n_{samples} \quad (3)$$

with $\omega_k = \frac{2\pi(k-1)}{n_{samples}\cdot t_{switch}}$. $Y(k)$ and $U(k)$ are the discrete Fourier transforms of the input and output signals averaged over all considered periods. The Fourier transforms were calculated as

$$X(k) = \sum_{n=1}^{n_{samples}} x(n)\cdot e^{-2\pi j\cdot \frac{(n-1)}{n_{samples}}\cdot(k-1)}, \quad k = 1...n_{samples}. \quad (4)$$

Figure 4 shows the ETFE calculated from periods 2-5 for both experiments. Moreover it shows a Bode plot of a fitted transfer function, see the next paragraph. It can be seen that both ETFE match very well. Naturally, they had been first calculated from periods 2-8. Since those did not differ from the shown ones, we concluded that 4 periods are enough for calculating the ETFE of this setup.
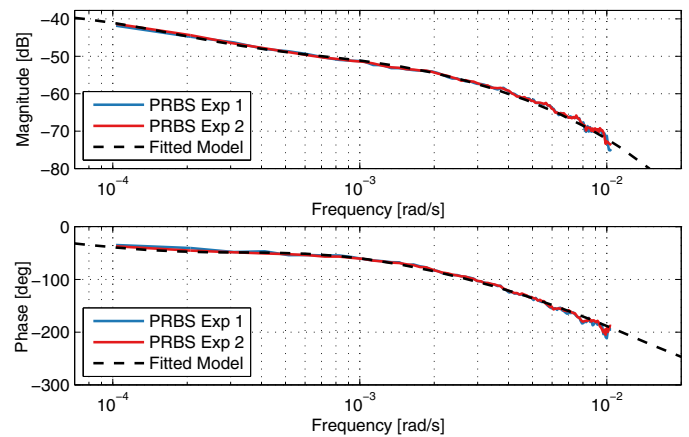

Fig. 4. Magnitude and phase plots of the ETFEs from two PRBS experiments and of a transfer function (see Equation (5)) fitted to the ETFEs.

Parametric Model Representation   For control purposes a parametric representation is needed. The fitting of a transfer function $G_{fit}(s)$ to the ETFEs was done manually. The resulting transfer function was

$$G_{fit}(s) = \frac{0.0132}{11800\cdot s + 1}\cdot(2800\cdot s + 1)\cdot\frac{1}{640\cdot s + 1}\cdot \frac{1}{(90\cdot s + 1)^2}\cdot\frac{1}{(40\cdot s + 1)}. \quad (5)$$

3.2 Identification Using a Relay Feedback

As an alternative identification approach we used relay feedback to determine the ETFE. A relay feedback controller always switches after passing the steady-state point resulting in a controlled oscillation that can be used to identify the frequency at which that plant has $-180°$ phase and the magnitude at this frequency. In combination with a lead/lag controller which effectively shifts the plant's $-180°$ phase frequency. This allows identifying any desirable point on the ETFE, see e.g. Smith and Doyle (1993). Since the relay's control signal as a function of the plant's output is piecewise constant with only one discontinuity, the input is almost uncorrelated to the plant's output noise. This justifies the calculation of the ETFE using

the previously described method. In the implementation, a relay with hysteresis was used to avoid potential instability due to noise at the switching point.

For every lead/lag setting the ETFE was calculated at the oscillation frequency, resulting in the data-points shown in Figure 5. It can be seen that they correspond very well to the ETFEs estimated in the PRBS experiments.
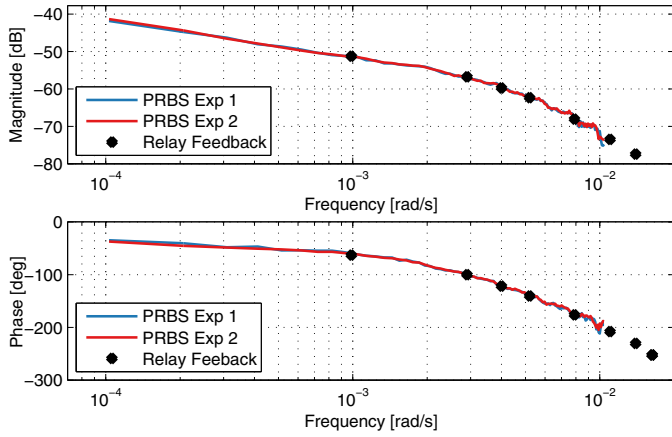

Fig. 5. Magnitude and phase plots of the ETFEs estimated from the two PRBS experiments and from the relay feedback experiment.

4. VALIDATION EXPERIMENT AND COMPARISON TO RC MODEL

In this section we show the results of a 134 h validation experiment consisting of heating power steps, ramps and PRBS-like fast signals. Using this data we assessed the predictive capabilities of several models: i) the identified model (5); ii) a physics based resistance-capacitance (RC) model of the room derived from construction data; iii) a modified version of ii) having an additional pole. The modification was motivated by a comparison of the identified and the RC model in frequency-domain which is also shown in this section. Last, we show by another PRBS experiment with fans in the room that the main source of the found difference are neglected room air mixing dynamics.

4.1 RC Model

The RC model was generated with the BRCM Toolbox [6] which is a free Matlab toolbox that generates (bi-)linear RC models of buildings for MPC from construction data, see Sturzenegger et al. (2014). The resulting model had 13 states representing the average room air temperature (one state) and the four walls', the floor's and the ceiling's layer temperatures (two states each). The output of the model was the operative room temperature, i.e. the average of the room air temperature and an area weighted average of the walls', floor's and ceiling's surface temperature. The inputs to the RC model were the ventilation air flow rate (fixed to 180 m³/h, see Section 2), the ambient temperature, T_{amb}, and the heater's power, $\dot{Q}_{heat}$. The floor and the ceiling as well as the west and east walls in direct contact with the heavy load-bearing walls (see Figure 1) were modeled

to have a constant temperature boundary condition. This temperature was set to 28 °C and was estimated as the average of the experimental room's past temperature and an assumed surrounding rooms' temperature. The north and south walls were modeled to have convective boundary conditions to the ambient air temperature T_{amb}. The only other model parameters which were not derived from the construction data were the convective coefficients. These were set [7] to 8 W/m²K.

4.2 RC Model Modification

Figure 6 shows the Bode plot of the identified model, of the original RC model (from heater power to operative temperature) and of the modified RC model (from heater power to the modified operative temperature). Clearly, the identified model and the original RC model differ significantly at higher frequencies. To compensate for this effect in the modified RC model (otherwise identical to the original RC model), another pole at $4 \cdot 10^{-4}$ rad/s was added to the output. In the time-domain this means that an additional state was added which was solely driven by the original model's output, influenced none of the other states and was considered as the modified model's output. The pole's frequency was fitted by hand. The modification is motivated on one hand by Figure 6 and on the other hand by the time-domain validation results of the following Section 4.3. Both show clearly that the RC model responds significantly faster to high frequency inputs than the measurements. As we show in Section 4.4 this stems mostly from not modeling mixing dynamics of the room's air.
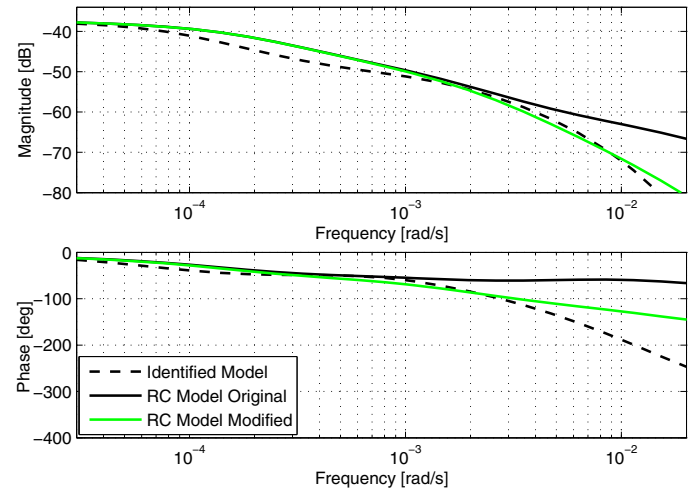

Fig. 6. Frequency-domain comparison of identified model, original RC model and modified RC model.

4.3 Validation Experiment

Figure 7 shows in the top plot the input signal, the measured T_{table} temperature as well as the outputs of the identified model, the original and the modified RC model. In the bottom plot, the differences between the measured and the model output temperature are plotted. In relation

---

[7] This is a standard value when the radiation heat transfer is considered also in the convective coefficient as it is the case in the chosen modeling approach.

to the peak to peak temperature change of around 12 °C, it is apparent that all models predict the temperatures reasonably well with an average and maximum error of roughly 0.5 °C (5 % of peak to peak) and 1.2 °C (10 %). Comparing the original to the modified RC model, the temperature and error trajectories are almost identical except for the high frequency part of the signal (around hour 120) where the error is significantly reduced in magnitude and fluctuation.
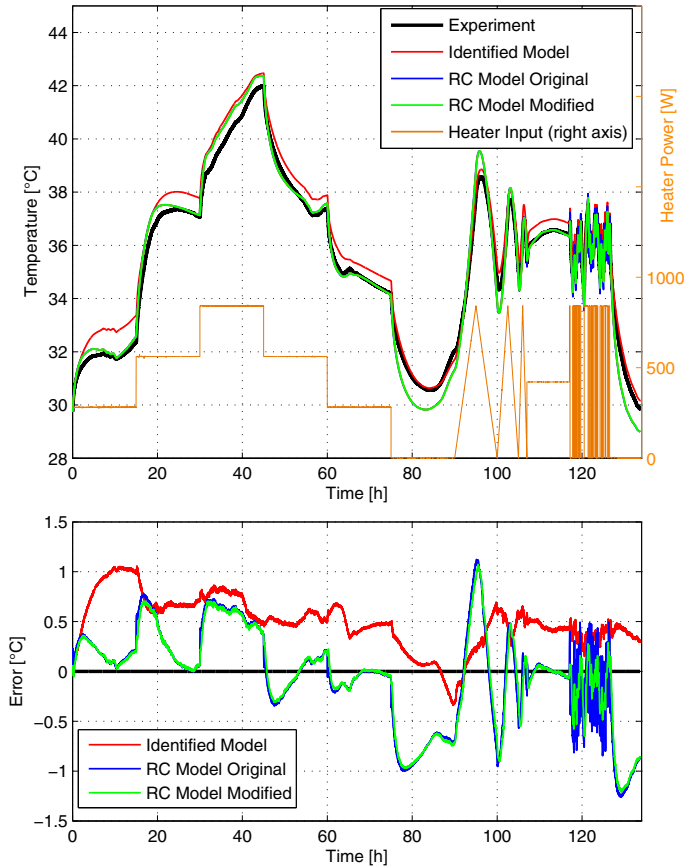

Fig. 7. Validation experiment. Upper plot: Experimental data and temperature trajectories predicted by the identified model, the original and the modified RC model. Lower plot: Errors (measured - model output) of all models.

4.4 Mixing Dynamics

Considering the discrepancy at high frequencies between the original RC model and the identified model shown in Figure 6, a likely cause seemed to be neglected air mixing dynamics. In building modeling, it is often assumed that the air of a zone has uniform temperature and hence that heating, for instance of the supply air, has immediate effect at all points within the room. Naturally this assumption is a simplification, in general because the heat exchange within the air is not instantaneous and hot air tends to rise. Moreover, in ventilated setups air paths (inlet to outlet) may shortcut much of the air volume. To investigate the magnitude of these effects and its influence on the identified transfer function, another PRBS experiment with the same heating trajectory as the first two was conducted. This experiment however had three

standard office fans in the room stirring the air. In Figure 8, we show a small part of the temperature trajectories of the first PRBS experiment from Section 3.1 and the same part of the experiment with the fans. Note the different temperature offsets. The mixing dynamics effect is apparent seeing the temperature differences between the sensors of up to 2.5 °C in the first experiment while in the second experiment the maximum discrepancy was just 0.4 °C. In Figures 9 and 10, we show the ETFEs of the
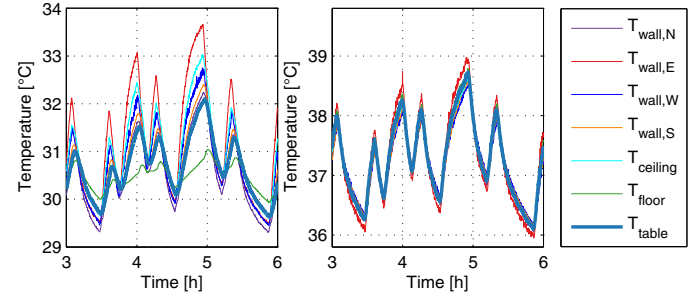

Fig. 8. Measurements of all room temperature sensors during the PRBS experiments. Left: PRBS experiment 1 (without fans). Right: PRBS experiment with fans in the room.

fastest ($T_{wall,E}$) and the slowest (T_{floor}) sensor as well as of T_{table} of the PRBS experiment with and without fans. Also the Bode plots of the identified and the original RC model are shown. Of course the Bode plot of the identified model coincides well with T_{table} in Figure 9 since it was the basis for the model fitting. In the same figure, large discrepancies between the three sensors' ETFEs can be observed. In Figure 10, two major observations can be made. First, all sensors now have almost identical ETFEs. Second, these ETFEs now coincide much better with the Bode plot of the original RC model. This indicates that the discrepancies between the sensors and the RC model actually were due to neglected mixing dynamics.
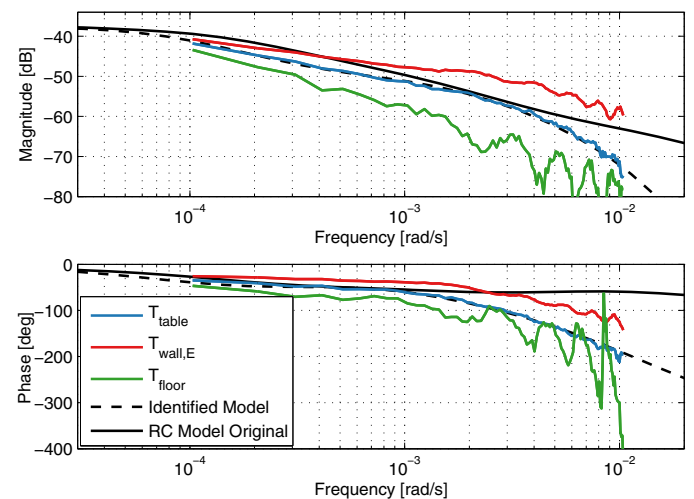

Fig. 9. Results of the PRBS experiment 1 (without fans in the room). ETFEs of T_{table}, $T_{wall,E}$ and T_{floor} as well as Bode plots of the identified and the original RC model.
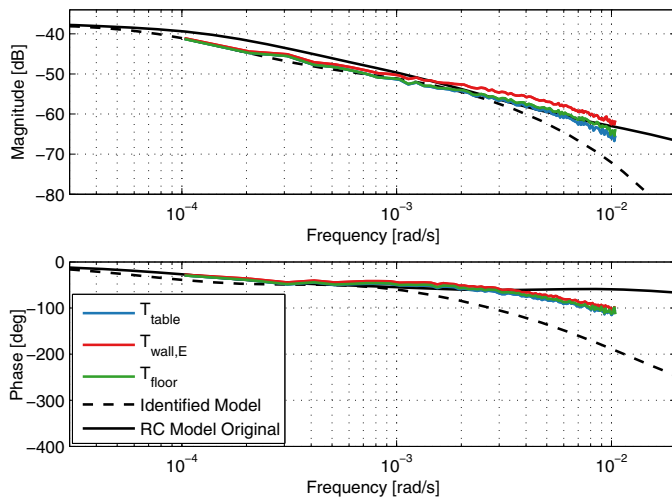
Fig. 10. Results of the PRBS experiment with fans in the room. ETFEs of T_{table}, $T_{wall,E}$ and T_{floor} as well as Bode plots of the identified and the original RC model.

5. DISCUSSION

Both applied identification methods showed very reproducible and closely matching results. A critical issue in a practical application is time efficiency. While the PRBS method identifies all points in one long experiment (in our case at least 3, ideally 5 periods of 17 h), the relay method can be used to subsequently identify single points[8] in much shorter experiments (several cycles at the frequency at which the system is to be identified). Unsurprisingly for such a thermal system, the ETFE turned out not to be very complex which suggests that only a few points may suffice for the identification of the whole system.

Both, the identified and the original RC model, showed a reasonable performance in predicting the room temperature measured by T_{table} during the 134 h validation experiment. The original RC model had higher high frequency gain. This behaviour was significantly damped by the additional pole in the modified RC model. Moreover, the pole significantly reduced the gap between the Bode plots of the identified and the RC model. The high frequency part of the validation experiment had a minimum switching time of 480 s. Since this is in the order of building MPC sampling times, this finding is meaningful in that context. The location of the pole was fitted to best reduce the discrepancy between the identified and the RC model. Naturally, there is in general no identified model available and the best pole position may lie at a different frequency. Nevertheless, this is a one-parametric approach for improving an RC model's fast dynamics in a standard ventilation setup. Since most other building systems are slower, their responses likely are insignificantly affected.

Comparing the results of the PRBS experiment with and without fans nicely showed that the discrepancy of the identified and the RC model stems from neglected mixing dynamics. The experiment with fans resulted in ETFEs

---

[8] Having no cooling device diminishes this advantage since the system must be first brought to steady-state conditions corresponding to 50 % of the maximum PRBS signal value.

which corresponded significantly better with the original RC model's Bode plot.

6. CONCLUSION

A well instrumented ventilated test room was used for identification experiments. Pseudo-random binary sequence (PRBS) and relay feedback based identification methods were applied to calculate an empirical transfer function estimate (ETFE). The relay feedback method employed a set of lead/lag controllers to identify the system at various frequencies. The PRBS method resulted in very reproducible results which coincided also well with the relay feedback results. A parametric model was fitted to the identified ETFE and was shown in a validation experiment to have an average and maximum error of roughly 0.5 °C (5 % of peak to peak) and 1.2 °C (10 %), respectively. A physics based RC model was generated and compared in frequency-domain to the identified model. At high frequencies the models were found to diverge. This was shown in a separate PRBS experiment including fans in the room to be mainly due to neglected air mixing dynamics. To compensate, an additional pole was added to the RC model's output. Both the original and the modified RC model were found to produce errors in the same range as the identified model. Moreover, the modified RC model was found to have in the high frequency part a much reduced error compared to the original RC model (otherwise almost identical). The improvement of the RC model from the additional pole is likely to be relevant in building MPC since it improves the model in a time range that is similar to typical control sampling times.

REFERENCES

Bengea, S.C., Kelman, A.D., Borrelli, F., Taylor, R., and Narayanan, S. (2014). Implementation of model predictive control for an hvac system in a mid-size commercial building. *HVAC&R Research*, 20(1), 121–135. URL http://www.tandfonline.com/doi/abs/10.1080/10789669.2013.834781.

Ma, Y., Borrelli, F., Hencey, B., Coffey, B., Bengea, S., and Haves, P. (2012). Model predictive control for the operation of building cooling systems. *IEEE Trans. on Control Systems Technology*, 20(3), 796–803.

Oldewurtel, F., Parisio, A., Jones, C., Gyalistras, D., Gwerder, M., Stauch, V., Lehmann, B., and Morari, M. (2012). Use of model predictive control and weather forecasts for energy efficient building climate control. *Energy and Buildings*, 45, 15–27.

Siroky, J., Oldewurtel, F., Cigler, J., and Privara, S. (2011). Experimental analysis of model predictive control for an energy efficient building heating system. *Applied Energy*, 88(9), 3079–3087.

Smith, R.S. and Doyle, J.C. (1993). Closed loop relay estimation of uncertainty bounds for robust control models. *Proc. 12th IFAC World Congress*, 9, 57–60.

Sturzenegger, D., Gyalistras, D., Gwerder, M., Sagerschnig, C., Morari, M., and Smith, R.S. (2013). Model Predictive Control of a Swiss Office Building. In *11th REHVA World Congress Clima 2013*.

Sturzenegger, D., Gyalistras, D., Semeraro, V., Morari, M., and Smith, R.S. (2014). BRCM Matlab Toolbox: Model Generation for Model Predictive Building Control. In *American Control Conference 2014 (accepted)*.